

Removal of the Amoxicillin from wastewater using Graphene Oxide; Thermodynamics and Kinetics Study

F. Iqbal & T. Mahmood

National Center of Excellence in Physical Chemistry, University of Peshawar Pakistan.

Corresponding Author email: tahiramahmood@uop.edu.pk

Abstract

Significant concerns are raised over pharmaceutical contamination in water bodies. The present article explores the redemption of Amoxicillin, a pharmaceutical micropollutant in wastewater discharged from hospitals. Graphene oxide (GO), derived from graphite powder, was applied using a modified Hummer method. Different analytical techniques, such as XRD, SEGM, FTIR, TGA, and Point of Zero Charge (PZC), were used to characterize the GO. Results showed that GO was an efficient adsorbent for removing Amoxicillin from wastewater samples prepared at laboratory scale. SEM exhibited that the Amoxicillin firmly deposited on the graphene oxide surface at pH 2 while lower at higher pH, showing that the removal was pH dependent. The adsorption isotherm fits the Langmuir model, showing maximum adsorption at 278K, with $X_m = 322.5 \text{ mg/g}$. The kinetics showed that adsorption favoured a pseudo second order model. The proposed mechanism of the process was reported.

Keywords: Pharmaceuticals, contamination, characterization, adsorption, kinetics, thermodynamics

1.0. INTRODUCTION

The consumption of human and veterinary pharmaceuticals has been increasing. Over the last ten years, research interest has expanded into the potential environmental impacts of pharmaceuticals in the environment. Pressure is exerted upon the environment due to extensive agriculture and industrialization. As diseases become more prevalent, the consumption of pharmaceuticals increases. Pharmaceuticals such as hormones and antibiotics have been detected for their presence in the environment [1]. Chiral pharmaceuticals are creating even more challenges for the well-being of ecosystems. The fate and effects of complex compounds such as chiral pharmaceuticals are still not known to quite an extent. There is a dire need for research, which needs to be done in this regard. Environmental pollution can be classified into air, water, and soil. Removal of pharmaceuticals in surface waters can be done by photo-transformation, biodegradation, hydrolysis, and partition to sediment. Their removal in wastewater treatment plants is mainly restricted to biodegradation and abiotic processes such as oxidation and sorption [2-5]. However, these processes are time-consuming and need a lot of capital investment. Novel approaches are required to design environmentally and economically friendly methods to address this challenge [3, 4-6]. Water is a necessity for life [7]. It is vital for all living organisms on Earth. Pollution has caused a severe impact on the quality of water available for human and animal consumption. Researchers have developed several technologies to address this challenge. However, these processes have been shown to report their limitations and disadvantages, e.g. chemical oxidation and ion exchange have reported low efficiency in removing trace amounts of pollutants from water samples. Thus, novel approaches are required for a comprehensive chemical and biological treatment of water bodies to make clean water available for consumption. Adsorption is a surface phenomenon. When a solution containing absorbable solute meets a solid with a highly porous surface structure, some solute molecules get deposited at the solid surface, forming the basis of separation by adsorption technology [8,9]. The metabolism of Antibiotics such as tetracycline is poor in humans and animals. They are not efficiently absorbed and intend to create leftovers in the environment because they are released in the unmetabolized form [10]. This has resulted in a need for sensing and subsequent elimination of these antibiotics from water. These antibiotics contaminate the natural living biota, such as soil and water. The residues of these antibiotics are present in environmental samples. Failure to detect these antibiotic residues in polluted samples doesn't mean these compounds aren't present or they don't persist in ecological habitats. The diversity in their biochemical properties makes it difficult to evaluate and detect. Chemical determination becomes difficult due to biodegradation, photodegradation, chelation, and chemical complexation. Liquid chromatography, mass spectrometry, solid phase extraction, and adsorption are usually employed to evaluate, determine, and estimate environmental samples [11].

In this research, adsorption was designed as an efficient methodology for detecting and removing one of Pakistan's highly-consumed antibiotics, Amoxicillin. Amoxicillin has been reported to be one of the potential contaminants in water bodies. It is categorized as Emerging Pollutants [12]. Morphologically, it has three aromatic rings with different functional groups such as amine, hydroxyl, ketone and carboxylic acid. Graphene is recently discovered and reported as a novel adsorbent material [13]. This material is explored for pollutant removal, specifically antibiotics from water. Hydrochemists investigate it for water purification. Morphologically, it is a single-layered graphite. Large quantities of oxygen atoms in epoxy, hydroxyl and carboxyl groups make it hydrophilic and can be applied in aquatic and biological environments for improvement.

It is reported that aromatic compounds can readily get adsorbed onto Graphene [11-13]. Various models have been designed and reported to investigate the adsorption behaviours of Graphene and its derivatives [14]. This article monitored the removal of *Amoxicillin* at the laboratory scale using kinetics and adsorption methods at several parameters to optimize the elimination of it from wastewater discharged from Hospitals.

2.0 MATERIALS AND METHODS

2.1. Reagents

All chemicals were used of analytical reagent grade and used without further purification. Amoxicillin Trihydrate was obtained from Merck. Co. Graphite Powder was bought from Aldrich, Germany. Di-ionized water was used with resistivity higher than 18M Ω cm.

2.2 Instrumentation

Shimadzu UV Visible spectrophotometer model 160-A was used for the spectroscopic studies. SEM (model JSM- 6490, JEOL) was used for SEM analysis. The X-ray diffractometry of the prepared sample was carried out using Cu-K α radiation at 40 KV voltage and 20 mA flow of current using a JEOL X-ray Diffractometer (JDX-7E) over a wide range of angles (25-80°). Thermogravimetric Analysis of the prepared samples was done using Perkin Elmer Model 6300. FTIR analysis was conducted using an infrared spectrophotometer (model SHIMADZU 8201 PC).

2.3. Preparation of Graphene Oxide

Graphene oxide was made from graphite powder using the modified Hummer method [15]. Graphite powder (2 g) was first oxidized by adding it into concentrated H₂SO₄ (12 mL), KMnO₄ (2.5 g), and P₂O₅ (2.5 g) at 80°C for 4.5 hrs. It was followed by dilution, filtering and washing. The mixture was diluted with 0.5 L water. This pre-oxidized graphite was added to cold concentrated H₂SO₄ (120 mL) with gradual KMnO₄ (15 g) addition under stirring while keeping the temperature below 20°C. This mixture was stirred at 35°C for 30 mins and then 90°C before further diluting, heating and stirring. After completing the reaction with 20 mL of 30% H₂O₂, the product was purified by filtration, HCl washing and dialysis. Exfoliation was achieved via sonication and centrifugation at 3000 rpm, and 16,000 rpm was used to collect the final residue for absorption testing [16].

2.4. Adsorption and Removal of Amoxicillin by Graphene Oxide

Batch adsorption experiments were carried out to study the effect of Adsorbent Dose, Contact Time, Solution pH, Temperature, and Initial Concentration of Amoxicillin Adsorption on Graphene oxide. A stock solution of Graphene oxide (200 ppm) was prepared. Out of this stock solution, 100 and 50 ppm of graphene oxide solutions were prepared using dilution. Similarly, an Amoxicillin stock solution (1000 ppm) was prepared. A series of dilutions ranging from 1 to 60 ppm were prepared from the stock solution. The solution pH was adjusted using 0.1 M hydrochloric acid or 0.1M sodium hydroxide. Solutions were incubated at different temperatures, i.e. at 278, 298, and 308K. After incubation, the suspensions were filtered. The suspensions were centrifuged at 200 rpm for 15 minutes. The filtered suspensions were then analyzed using a UV UV-visible spectrophotometer. The wavelength chosen was 270nm. Amoxicillin shows maximum adsorption at 270 nm when present in aqueous medium. The amount of Amoxicillin adsorbed on graphene oxide was measured based on the difference in the solution's initial and final Amoxicillin concentration. Orion pH meter (710 A) was used for noting the solution pH

The Maximum adsorption capacity was calculated from the equation:

$$X = (C_i - C_e) \times V / 1000 \times m$$

Where X= amount of Amoxicillin adsorbed (mg.g⁻¹)

C_i= Initial Amoxicillin Concentration (mg.g⁻¹)

C_e= Equilibrium Amoxicillin concentration (mg.g⁻¹)

V= volume of Amoxicillin solution (mL)

m= Adsorbent Mass (g)

3.0. RESULTS AND DISCUSSION

3.1 Characterization of Graphene Oxide

The GO is characterized using FTIR, SEM, XRD and TGA (Fig.1-5). Scanning Electron Microscopy revealed a single-layered structure (Fig. 1) before adsorption, while Fig. (2) showed SEM after adsorption, where it was observed that the surface was fully covered by adsorbate.

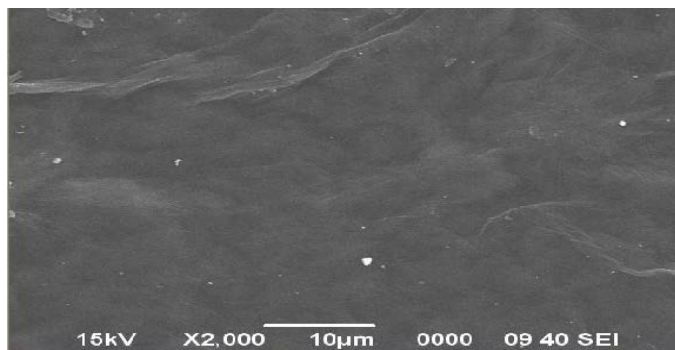


Figure 1: Scanning Electron Microscopy of Graphene oxide before adsorption.

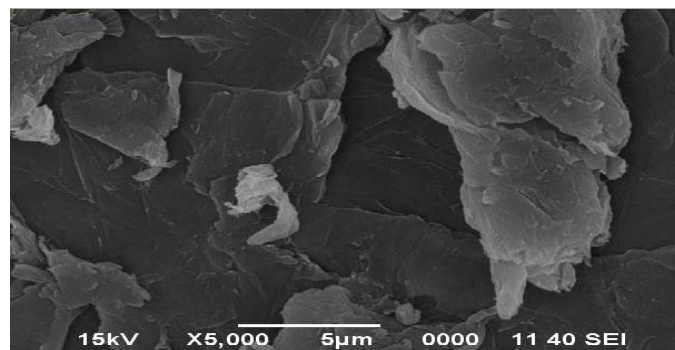


Figure 2: Scanning Electron Microscopy of Graphene Oxide after adsorption.

The FTIR spectra (Fig.3) showed the characteristic peaks of the hydroxyl group (OH) at 3400 cm^{-1} , Carbonyl group (CO) at 1729 cm^{-1} ; the peak corresponds to 1388 due to $-\text{OH}$ bending vibrations, $-\text{C}-\text{O}-\text{H}$ in-plane bending vibrations, $-\text{CH}_3$ out-of-plane bending vibrations, $-\text{CH}_2-$ wagging and twisting vibrations, COH (1224 cm^{-1}), and CO (1047 cm^{-1}) functional groups. It showed the oxygen-containing groups introduced into the graphene structure that play a significant role in removal through adsorption. The X-RD pattern displayed a peak centred at $2\theta = 11.08$, corresponding to the (002) inter-planar spacing of 8.0 \AA (Fig.4).

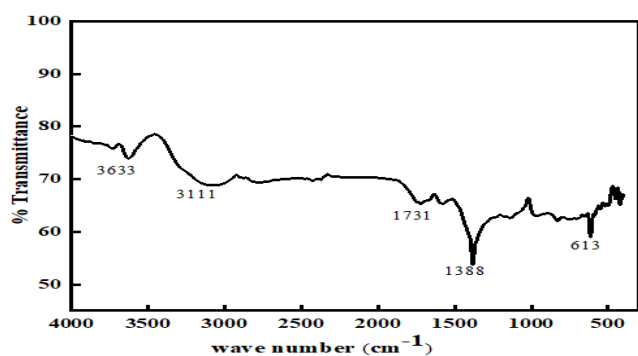


Figure 3: FTIR spectrum of graphene oxide

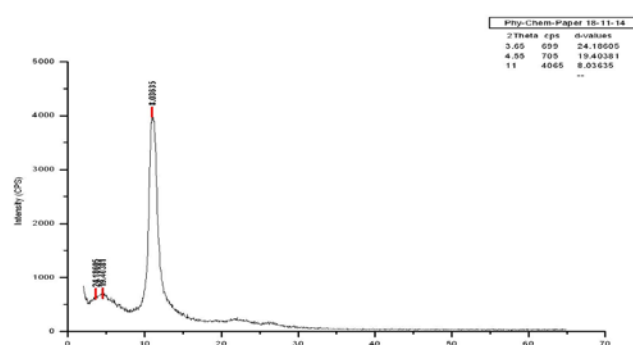


Figure 4: X-RD spectrum of graphene oxide sheet made in the laboratory

Thermogravimetric Analysis (TGA) was conducted to evaluate the thermal stability of the synthesized graphene oxide (GO). The TGA curve for GO, shown in Fig. (5), indicates two significant weight losses at 230°C and 700°C , corresponding to the removal of oxygen-containing functional groups and carbon oxidation, respectively. The percentage weight losses at 230°C and 700°C were 69% and 78%, respectively, suggesting that beyond 700°C , the composite material achieves thermodynamic stability without further degradation. This stability enhances its suitability for adsorption applications, including the adsorption of Amoxicillin, which is similar to the earlier reports[17].

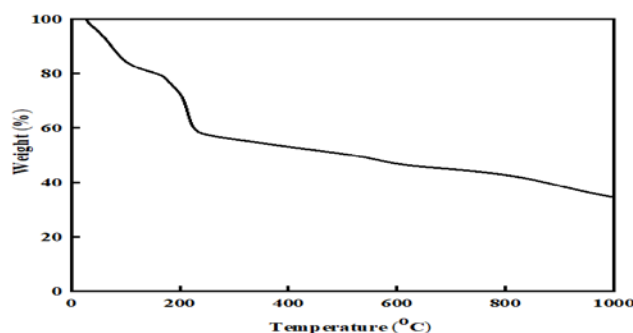


Figure 5: Thermogravimetric curve of the prepared graphene

3.2 Adsorption isotherms of Amoxicillin on Graphene Oxide

Removal of Amoxicillin from wastewater was investigated through three adsorption isotherms (Langmuir, Freundlich, and DR models) [18] to evaluate the adsorption capacity of GO. C_e (mg/g) indicates the equilibrium adsorption concentration once maximum adsorption is achieved. X_e (mg/g) is the equilibrium adsorption capacity of graphene oxide and the difference between the initial (C_i) and final concentration (C_e) is caused by the per unit weight of the adsorbent. As can be seen, adsorption is highly affected by an increase in temperature. The mathematical representation of the three models is given below:

$$X_e = 1/K_b X_m + C_e / X_m \quad \text{_____ (1)}$$

$$\text{Log } X_e = \text{Log } K_f + 1/n \text{ log } C_e \quad \text{_____ (2)}$$

$$\ln X_e = \ln X_m - K\varepsilon^2 \quad \text{_____ (3)}$$

where K_b , K_f , and K are the constants for Langmuir, Freundlich, and DR models, respectively, and n is the Freundlich linearity index. Langmuir's model (Eq. 1-3) is ideal for showing good adsorbent surface and monolayer adsorption [19]. For empirical speculation, Freundlich is used where, whereas DR model is used to evaluate the process's adsorption energy (E) (Fig.6-9). The values of adsorption enthalpy (ΔH), entropy (ΔS) and Gibbs free energy (ΔG) (Eq.4 & 5) were calculated using:

$$\ln K_b = \Delta S/R - \Delta H/RT \quad \text{_____ (4)}$$

$$\Delta G = -RT \ln K_b \quad \text{_____ (5)}$$

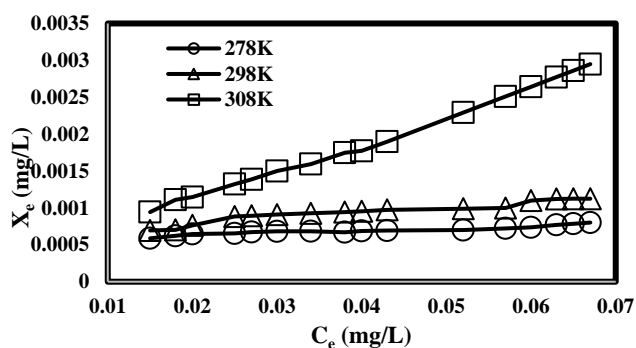


Figure 6: Langmuir Adsorption isotherms of Amoxicillin on GO

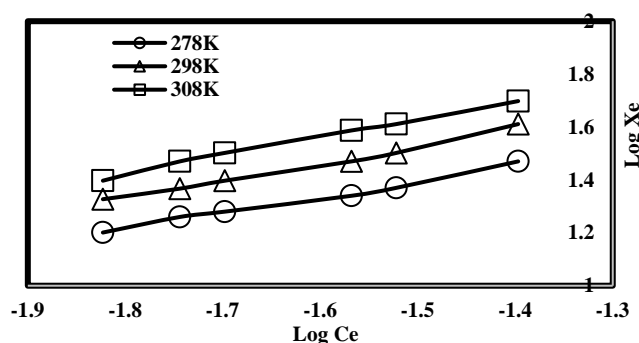


Figure 7: Freundlich Adsorption isotherms of Amoxicillin on GO

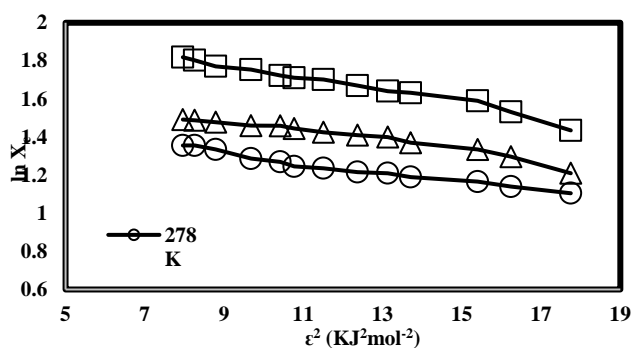


Figure 8: DR model Adsorption isotherms of Amoxicillin on GO

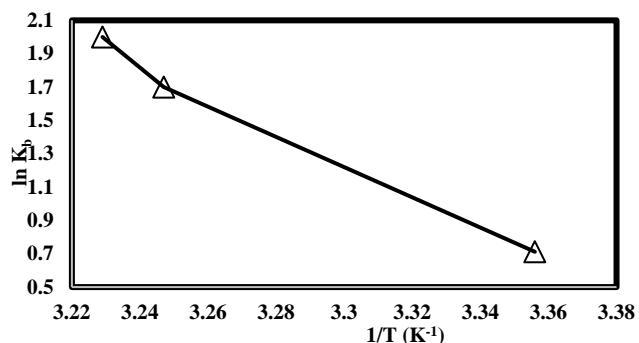


Figure 9: A plot of $\ln K_b$ vs T^{-1} for estimating thermodynamic parameters.

The results of fitting these models are shown in Fig.(6-9), and the fitting parameters are listed in Table (1). As mentioned earlier, the Langmuir model fits the data well, whereas the DR model is used to evaluate the thermodynamic parameters. Notably, adsorption decreases with the rise in temperature, showing the endothermic nature of the process. Although Langmuir mostly fits the data well, it has limitations at higher concentrations. The maximum adsorption capacity from the Langmuir model was 322.5 mg/g at 278 K, which considerably lowered with temperature. The DR model gives insight into the porosity and free energy of the process, which also decreases with the rise in temperature.

Temperature	Langmuir			Frendlich			Dubinin- Radushkevich (DR)		
	X_m (mg/g)	K_b (L/mg)	R^2	n	K_f	R^2	X_m (mg/g)	K ($\text{mol}^2\text{kg}^{-2}$)	E (kJ/mol)
278	322.5	5.16	0.99	1.81	164	0.98	4.67	0.025	4.46
298	135.1	12.5	0.99	1.68	264	0.99	5.57	0.026	4.38
308	26.38	100	0.99	1.45	456	0.99	8.08	0.034	4.00

Table 1: Adsorption of Amoxicillin on Graphene Oxide (Langmuir, Freundlich and DR isotherm fitting parameters)

The adsorption mechanism of Amoxicillin onto Graphene Oxide needs further investigation [19,20]. Generally, aromatic rings get adsorbed onto graphene oxide by $\pi - \pi$ stacking, which shows non-covalent interaction between the π bond and aromatic ring. The pH of the system varied between 2 to 11 at temperatures of 298K and 308K (Fig.10). However, in this study, pH played a significant role, and adsorption was greatly influenced by the pH of the medium, similar to the earlier reports[21-25]. Three different concentrations, 20 ppm, 30 ppm, and 50 ppm, were taken. The maximum adsorption of the molecule is shown at pH 2, which decreases steadily with the increase in the system's pH.

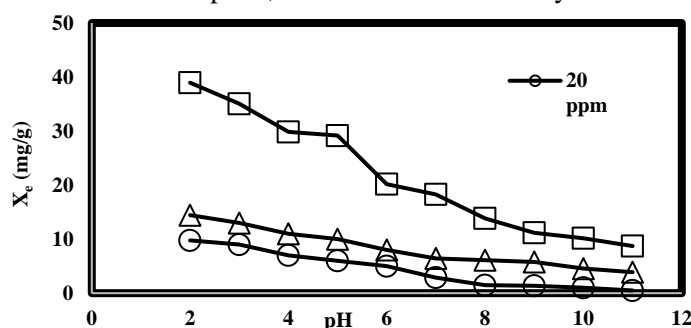


Figure 10: Effect of pH on the adsorption of Amoxicillin on Graphene oxide at 298K and 308K

and unfavourable at alkaline pH. The greater Amoxicillin uptake may be associated with the electrostatic attraction between the surface of the Graphene Oxide and Amoxicillin molecule. The PZC value determined for the prepared adsorbent is 2. This means that below this pH, the surface is positively charged. The adsorption of the molecule is associated with the ionization of the carboxylic acid group attached to the Amoxicillin molecule, which has a pKa value of 2.68. The carboxylic acid group releases the H⁺ ion into the solution, leaving behind the negative charge on the oxygen molecule bonded to the Amoxicillin molecule. This electrostatic force of attraction facilitates the adsorption of the Amoxicillin molecule on the Graphene Oxide surface. This phenomenon occurs due to the ionization of its functional groups identified as carboxyl (pKa = 2.68), amine (pKa = 7.49) and phenolic hydroxyl (pKa = 9.63). The protonation for both Amoxicillin groups at low pH enhances the adsorption mechanism. The initial pH at which ΔpH crosses zero was taken as the PZC of the sample. The other functional groups, i.e. amine (pKa = 7.49) and phenolic hydroxyl (pKa = 9.63), do not play a significant role in adsorption. Several researchers have reported a similar behaviour pattern in their work. When pH increases, it suppresses the release of H⁺ ions into the medium; adsorption is not favourable at higher pH. Activated Carbon and Bentonite showed similar behaviour during the investigation of Amoxicillin removal [26-30]. Modified bentonite was used by Rahardjo et al.[25] for the Amoxicillin adsorption, a pH range from 3-7 promoted the adsorption rate [26-30]. Another parameter which plays a critical role in adsorption is the electrostatic force of attraction. The phenolic hydroxyl group is believed to create π - π stacking, as reported in the literature, where the tetracycline class of antibiotics are adsorbed on graphene oxide owing to π stacking.[31-36].

3.3. Adsorption kinetics of Amoxicillin on Graphene Oxide

For this study, the effect of contact time was studied. The effect of contact time on Amoxicillin adsorption on GO was studied at various time intervals from 1 to 300 minutes [31]. It was evident that Amoxicillin adsorption rises with the increase in the contact time until equilibrium is attained (Fig.11). Adsorption equilibrium for Amoxicillin is rapidly achieved within the first 100 minutes of the period, showing the availability of active surface sites for adsorption. At 278K, equilibrium is established quickly. Furthermore, Amoxicillin adsorption increases with temperature, indicating the endothermic nature of the adsorption process [18-20].

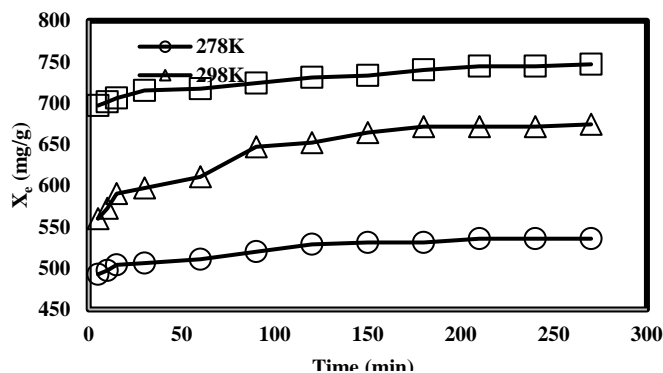


Figure 11: Effect of contact time on the adsorption of Amoxicillin on Graphene Oxide

The kinetic data was analyzed using pseudo-1st-order and pseudo-2nd-order models to determine the reaction rate. The non-linear forms of these models are given below:

$$\text{Log}(X_e - X_t) = \text{log } X_e - k_1/2.303 \quad (6)$$

$$t/X_t = 1/k_2 X_e^2 + 1/X_e t \quad (7)$$

Where k_1 (min^{-1}) and k_2 ($\text{g} \cdot \text{min}^{-1} \cdot \text{mg}^{-1}$) are the pseudo 1st order and pseudo 2nd order rate constants, respectively, the R^2 values for the pseudo 2nd order model are higher than the pseudo 1st order model (Eq. 6 & 7). The data aligns more closely with the pseudo-second-order model than the pseudo-first-order model. This shows that the chemical adsorption is the rate-limiting step.

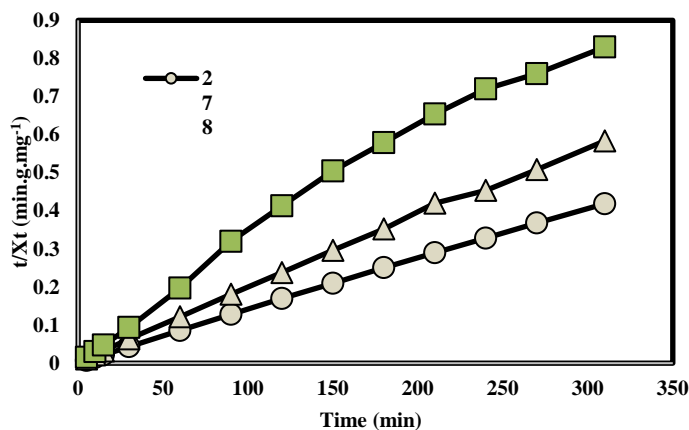


Figure 12: Pseudo second-order plot for the adsorption of Amoxicillin on GO.

The values of rate constants obtained from the pseudo-second-order kinetic model for Amoxicillin adsorption on Graphene Oxide were 0.0004, 0.0004, and 0.0005 ($\text{g} \cdot \text{min}^{-1} \cdot \text{mg}^{-1}$) at 278, 298, and 308K, respectively (Fig.12). The values of experimental X_e were 535.8, 674.4, and 747.2 (mg/g) which were close to the calculated values of X_e , i.e. 526.3, 769.2, and 1000 ($\text{mg} \cdot \text{g}^{-1}$) (Table 3) similar to the earlier reports[32-35]

Adsorbent	Temperature (K)	Experimental X_e [mg/g]	Calculated X_e [mg/g]	K_2 [g min ⁻¹ mg ⁻¹]	R^2
Graphene Oxide	278	535.8	526.3	0.0004	0.99
	298	674.4	769.2	0.0004	0.98
	308	747.2	1000	0.0005	0.99

Table 2: Pseudo-second-order kinetic parameters for the adsorption of Amoxicillin on Graphene Oxide

Activation energy is the minimum energy required for a chemical reaction to occur. The reactant molecules get close and come together, and the chemical bonds are stretched, broken, and formed in the product formation [36,37]. The system's energy increases to a maximum. The energy drops down when the product is formed. This energy is the variation between the maximum and the minimum i.e the energy barrier needed to overcome how the reaction rate varies with the temperature. These are expressed in kilojoules per mole. An activation energy more significant than 200 kJ/mol suggests that bonds have been completely broken and a transition state is formed. The energy of activation (E_a) was determined from the rate constant values calculated at different temperatures using the equation (8).

$$\ln k_2 = \ln A - \frac{E_a}{RT} \quad (8)$$

Where k_2 is the rate constant derived from the pseudo 2nd order kinetic equation, A is the Arrhenius frequency factor, T and R are the absolute temperature and universal gas constant, respectively. A plot of $\ln k_2$ versus $1/T$ (Fig. 13) showed a straight line with a coefficient of correlation (R^2) of 0.99 (Table 3). The energy of activation calculated from the straight line obtained is 41.57 kJ/mol. The energy of activation reveals the endothermic nature of the process. The positive activation energy values indicate that the reaction rate correspondingly increases with the rise in temperature, which is comparable (Table 4) to the earlier investigation by [38,39].

Temp [K]	ΔG [kJ/mol]	ΔH [kJ/mol]	ΔS [J/mol/K]	R^2
278	-3.79			
298	-6.26	78.25	268.36	0.99
308	-11.7			

Table 3: thermodynamic parameters for the adsorption of Amoxicillin on Graphene Oxid

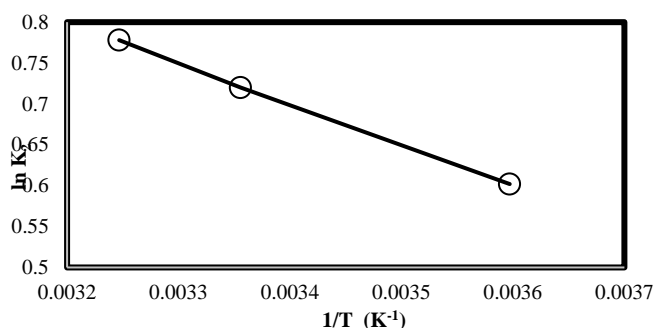


Figure 13: plot of $\ln K_2$ vs T^{-1} for the adsorption of Amoxicillin on Graphene Oxide

Adsorbent	E_a (kJ/mol)	R^2
Graphene Oxide	41.57	0.99
Sewage sludge-derived adsorbents (ACZn ₂)	21.41	Gupta and Garg [41]
Sewage sludge-derived adsorbents (ACZn _{2.5})	12.65	

Table 4: Comparison of the Activation Energy of various adsorbents in kJ/mol

The positive value indicates the reaction rate increases with the temperature rise. A comparison of activation energies of various adsorbents shows that graphene oxide is an excellent potential adsorbent for water purification[37-38]. The literature shows the activation energies for adsorbents derived from other sources, such as sewage sludge[41].

4. Conclusion:

In the present work, Graphene oxide was used as an adsorbent for Amoxicillin from aqueous solutions. It showed good adsorption capacity because of its hydrophilicity, inert nature and high surface area. Graphene oxide showed favourable adsorption capacity and efficient adsorption energy. The mechanism of the process was greatly influenced by pH of the medium. The removal through adsorption was pH-dependent. Adsorption kinetics showed the best fit for pseudo second order, while Langmuir isotherm fit the data well.

Acknowledgment

Authors acknowledge the Chairperson of the Department of Chemistry and Dean of the Faculty of Science for facilitating at the time of research conduction.

References

1. O.A. Jones, A. H., Voulvoulis, N., & Lester, J. N. *Crit.l Revs. Toxicol.* 34(4), 335–350, (2004).
2. S. Canonica, Meunier, L., Gunten, U.V. *Water Res.* 42, 121-128, (2004).
3. F. Cecen, Gul.G. *Int. J. Environ. Sci. and Tech.*,18, 327-340, (2021).
4. K. Beijer, Bjorlenius, B., Shaik,S., Lindberg, R.H., Bronstorm, B., Brandt,I. *Chemosphere*, 176, 342-351, (2017).
5. M. Horsing, Leddin, A., Grabic,R., Fick, J., Tysklind, M., Jansen, J,L,C., Anderson,H.R. *Water Res*, 45, 4472-4480, (2011).

6. T. G. Bean, Bergstrom, Ed., Thomas, O. T., Wolf, A., Bartl, P., Eaton, B., Boxall, A.B.A. *Environ. Manag.* 58,707-720, (2016).
7. I. Friddreksson, *Universal J. of Psychol.* 4(4), 178-183, (2016).
8. Ali, I., & Gupta, V. K. *Nat. Protoc.* 1(6), 2661–2667, (2007).
9. M. A. Alaei Shahmirzadi, Hosseini, S. S., Luo, J., & Ortiz, I. *J. Environ. Manag.* 215, 324–344, (2018).
10. R. Daghri, Drogui, P. *Environ Chem Lett*, 11, 209-227, (2013).
11. K. K. Saudi, Kumar, M., Singh, D.K. *JPWE*, 39, 101858, (2021).
12. M. Godoy, & Sánchez, J. *Antibiot Mat. Healthcare*, 221–230, (2020).
13. G. Z. ZKyzas, Deliyanni, E.Z., MAtis, K.A. *JCTB*, 165-327, (2014).
14. K.A. Mkhoyan, Countryman, A. W., Silcox, J., Stewart, D. A., Eda, G., Mattevi, C., Chhowalla, M. *Nano Lett.*, 9(3), 1058–1063, (2009).
15. L. Shahriari, Athawale, A, A. *Int. J. Ren. Energy Env. Eng.* ISSN 2348-0157, Vol. 02(01), (2014).
16. J. Chen, Yao, B., Li, C., & Shi, G. *Carbon*, 64, 225–229, (2013).
17. B. Lesiak, B., Stobinski, L., Malolepszy, A., Mazurkiewicz, M., Kövér, L., & Tóth, J. *J. Electron Spectros. Relat. Phenomena*, 193, 92–99, (2014).
18. J.Y. Juang Yeo, Khaurdini, D.S., Soetarejdo, F.E., Waworuntu, G.L., Ismadji, S., Putranto, A., Putranto, A., Sunarso, J. *S.Afr. J. Chem. Eng.* 43, 38-45, (2023).
19. J. A. Veith, Sposito, G. *Soil Sci. Soc. Am. J.*, 41(4), 697, (1977).
20. Y. Gao, Li, Y., Zhang, L., Huang, H., Hu, J., Mazhar Shah, S., Su, X. *J. Colloid. Interface Sci.* 368, 540-546, (2012).
21. R. Malarvizhi, Ho, Y.S. *Desalination*. 264(1-2), 97–101, (2010).
22. T. Ward, M., Getzen, F. M. *Env. Sci. Technol.* 4(1), 64–68, (1970).
23. J. J. M. Órfão, Silva, A. I. M., Pereira, J. C. V., Barata, S. A., Fonseca, I. M., Faria, P. C. C., & Pereira, M. F. R. *J. Colloid. Interface Sci.* 296(2), 480–489, (2006).
24. J. Martin, Orta, M.D.M; Medina Carrasco, S; Santos, J.L; Aparicio, I; Alonso. E. *Environ Res.* 164, 488-494, (2018).
25. A.K. Rahardjo, Susanto, M. J. J., Kurniawan, A., Indraswati, N., Ismadji, S., *J Hazard. Mater.* 190, 1001-1008, (2011).
26. Z. Jeirani, Niu, C.H; Sultan, J. *Rev Chem Eng.* 33(5), 491-522, (2017).
27. E. K. Putra, E.K., Pranowo, R., Sunarso, J., Indraswati, N., & Ismadji, S. *Water Res.*, 43(9), 2419–2430, (2009).
28. G. Moussavi, Alahabadi, A., Yaghmaeian, K., Eskandari, M. *Chem. Eng. J.* 217, 119–128, (2013)
29. H. Liu, Hu, Z., Liu, H., Xie, H., Lu, S., Wang, Q., & Zhang, J. *RSC Advances*, 6(14), 11454–11460, (2016).
30. S. Ahmadi, Ghosh, S., MAlloum, S., Sillanpaa, M., Igwegbe, C.A., Ovuroye, P.E., Ighalo, J.O. *Ind. Chem. Eng.* 66(1), 1-14, (2024).
31. L. Sellaoui, Lima, E. C., Dotto, G. L., & Lamine, A. B. *J. Mol. Liq.* 234, 375–381, (2017).
32. C.W. Gray, McLaren, R.G., Roberts, A.H.J., Condorn, L, M. *Aust. J. Soil Res.* 36 (2), 199-216, (1998).
33. H. Fu, Li, X., Wang, J., Lin, P., Chen, C., Zhang, X., Suffet, I. H. *J. Environ. Sci.* 56, 145–152, (2017).
34. N. Genç, Dogan, E. C. *Desalin Wat. Treat.* 53(3), 785–793, (2013).
35. S. H. Kim, Shon, H.K., Ngo, H.H. *J. Ind. Eng. Chem.* 16(3), 344–349, (2010).
36. M.J. Ahmed, *Review. Environ. Toxicol. Pharmacol.* 50, 1–10, (2017).
37. H.S. Taylor, *J. Am. Chem. Soc.* 53(2), 578–597, (1931).
38. M. Menzinger, Wolfgang, R. *Angewandte Chem Int. Eng.* 8(6), 438–444, (1969).
39. C. H. Wu, *J. Hazard. Mat*, 144(1-2), 93–100, (2007).
40. S. Agnihotri, Rood, M.J., Rostam-Abadi, M. *Carbon*, 43(11), 2379–2388, (2005).
41. A. Gupta, Garg, A., *Clean Techn Environ Policy.* 17, 1619-1631, (2015).

Received: 21th September 2024Accepted: 28th October 2024